

Received: 24.06.2023

Accepted: 03.03.2024

Research Article

QSAR/ANN approaches and molecular docking applied to calcium channel blockers

Siham Aggoun^a, Salah Belaidi^{a,1}, Lazhar Bouchlaleg^a, Hassan Nour^b, Oussama Abchur^b, Samir Chtita^{b,2}, Muneerah Mogren Almogren^c, Majdi Hochlaf^{d,3}

^aMohamed Khider University of Biskra, 07000, Biskra, Algeria

^bHassan II University of Casablanca, B.P. 7955, Casablanca, Morocco

^cKing Saud University, Riyadh 11451, Kingdom of Saudi Arabia

^dGustave Eiffel University, 5 Boulevard Descartes, 77454, Champs, France

Abstract: Dihydropyridines (DHPs) have emerged as one of the most commonly used families of drugs for treating various diseases related to heart and blood vessels. In this study, artificial neural networks (ANNs) and multiple linear regression (MLR) were applied to construct robust Quantitative Structure-Activity Relationship (QSAR) models modeling the biological activity of calcium channel blockers derived from 1,4-dihydropyridine. Quantum descriptors were calculated using the Density Functional Theory (DFT) with the B3LYP functional and the 6-31G+(d,p) base level. The predicted data derived from the developed models (ANN and MLR) are in perfect agreement with those derived from experiments. Furthermore, the molecular docking approach was applied to gain insights into the interaction mechanism of the investigated ligands and the target receptor, and to quantify their binding energies. The study also included the assessment of drug likeness to predict the behavior of the analyzed compounds in the human body. These computational methods have the potential to accelerate the discovery and development of new drugs, thereby revolutionizing the pharmaceutical industry.

Keywords: QSAR, Artificial Neural Network, DFT, Molecular Docking, Calcium Channel Blockers, Dihydropyridine.

1. Introduction

The dihydropyridine (DHP) family is a group of heterocyclic molecules based on pyridine. The total synthesis of the 1,4-dihydropyridine (DHP14) molecule was carried out by Hantzsch, a hundred years ago [1].

In recent years, researchers have tested and approved that DHP14 derivatives have significant biological activities and medical scientists have introduced them into clinical medicine for a wide variety of biological targets, for example as bronchodilators, vasodilators, anti-diabetics, anti-tumors, anti-inflammatories [4-12].

Over time, DHPs have become one of the most used families of drugs to treat various diseases related to the heart and blood vessels. [13-15]. These compounds act as calcium channel blockers (Ca^{2+}) which are also called (CCBs), so they are calcium channel antagonists, which disturb the fluidity of Ca^{2+} in the calcium channels. [3,16]. The most commonly used DHP14 are felodipine, clevidipine, benidipine, isradipine, nitrendipine, nifedipine [17,18], their structures are illustrated in Fig.1. The application of computational methods, such as QSAR modeling, molecular docking, and drug likeness, has shown great potential in accelerating

¹ Corresponding Authors

e-mail: prof.belaidi@gmail.com

² Corresponding Authors

e-mail: samir.chtita@univh2c.ma

³ Corresponding Authors

e-mail: majdi.hochlaf@univ-eiffel.fr

Siham Aggoun, Salah Belaidi, Lazhar Bouchlaleg, Hassan Nour, Oussama Abchir, Samir Chtita, Muneerah Mogren Almogren, Majdi Hochlaf

the discovery and development of new drugs. These approaches have the ability to revolutionize the pharmaceutical industry by providing reliable predictions and insights into ligand-protein interactions. modern works have used artificial neural network methods to build QSAR models with selective predictivity [19].

We found in the literature numerous QSAR analyzes on DHP14 analogues, which target the

discovery of new calcium channel blockers. In 2003, Safarpour et al [20] have carried out several QSAR studies, using quantum computing methods. In 2004, Hemmateenejad et al. [15] applied the GA-MLR and PC-GA-ANN techniques to model the CCB activity of the nifedipine analogue. In the year 2005, Yao et al. [21] used the LSSVM method to find selective models of a set of DHP14 inhibitors.

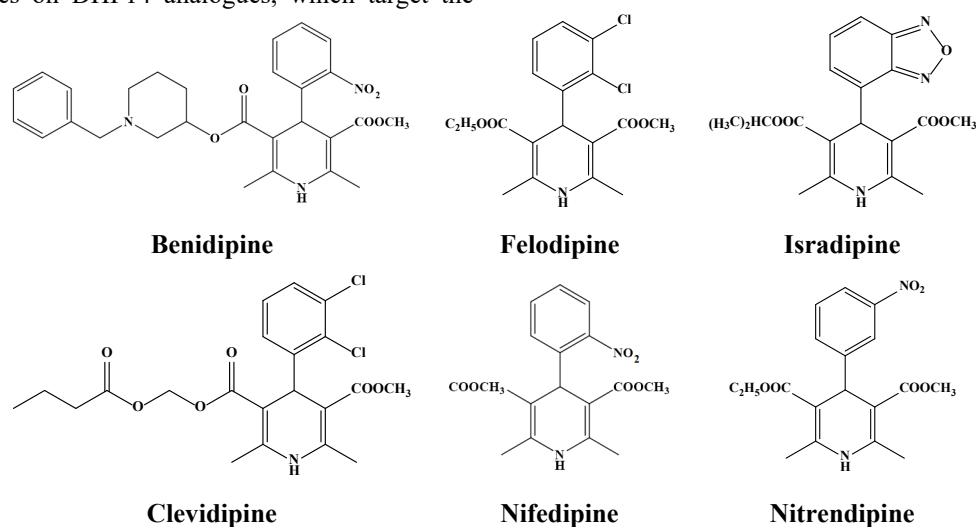
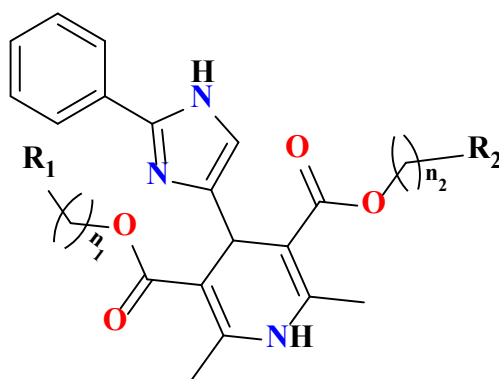


Fig. 1. Structures of the main DHP14.



Scheme 1. Structures of DHP14 derivatives under study.

Table 1. Structures of Ligands.

N	R ₁	n ₁	R ₂	n ₂	Molecular Formula	IC ₅₀ / mmol/l	pIC ₅₀
1*	C ₆ H ₁₁ ^a	0	C ₆ H ₁₁ ^a	0	C ₃₀ H ₃₇ N ₃ O ₄	3.02×10 ⁻¹⁰	9.52
2	C ₆ H ₁₁ ^a	1	C ₆ H ₁₁ ^a	1	C ₃₂ H ₄₁ N ₃ O ₄	3.60×10 ⁻¹¹	10.44
3	C ₆ H ₁₁ ^a	2	C ₆ H ₁₁ ^a	2	C ₃₄ H ₄₅ N ₃ O ₄	1.79×10 ⁻¹¹	10.74
4	C ₆ H ₁₁ ^a	3	C ₆ H ₁₁ ^a	3	C ₃₆ H ₄₉ N ₃ O ₄	1.20×10 ⁻¹¹	10.92
5	C ₆ H ₁₁ ^a	4	C ₆ H ₁₁ ^a	4	C ₃₆ H ₄₉ N ₃ O ₄	6.43×10 ⁻¹⁰	9.19
6	C ₅ H ₉ ^b	3	C ₅ H ₉ ^b	3	C ₃₄ H ₄₅ N ₃ O ₄	2.79×10 ⁻⁹	8.55
7*	C ₆ H ₅	1	C ₆ H ₅	1	C ₃₂ H ₂₉ N ₃ O ₄	5.61 ×10 ⁻¹⁰	9.25
8*	C ₆ H ₅	2	C ₆ H ₅	2	C ₃₄ H ₃₃ N ₃ O ₄	4.52 ×10 ⁻¹⁰	9.34
9	C ₆ H ₅	3	C ₆ H ₅	3	C ₃₆ H ₃₇ N ₃ O ₄	9.72 ×10 ⁻¹¹	10.01
10	C ₆ H ₅	4	C ₆ H ₅	4	C ₄₀ H ₄₅ N ₃ O ₄	6.42 ×10 ⁻¹⁰	9.19
11	C ₆ H ₅	5	C ₆ H ₅	5	C ₄₀ H ₄₅ N ₃ O ₄	8.91 ×10 ⁻⁸	7.05

Siham Aggoun, Salah Belaidi, Lazhar Bouchlaleg, Hassan Nour, Oussama Abchir, Samir Chtita, Muneerah Mogren Almogren, Majdi Hochlaf

12	C ₆ H ₁₁ ^{a)}	0	CH ₃	0	C ₂₅ H ₂₉ N ₃ O ₄	1.75 × 10 ⁻¹⁰	9.75
13	C ₆ H ₁₁ ^{a)}	0	CH ₂ CH ₃	0	C ₂₆ H ₃₁ N ₃ O ₄	8.45 × 10 ⁻¹⁰	9.07
14	C ₆ H ₁₁ ^{a)}	1	CH ₃	0	C ₂₆ H ₃₁ N ₃ O ₄	2.80 × 10 ⁻⁹	8.55
15*	C ₆ H ₁₁ ^{a)}	1	CH ₂ CH ₃	0	C ₂₇ H ₃₃ N ₃ O ₄	1.32 × 10 ⁻⁹	8.88
16	C ₆ H ₁₁ ^{a)}	2	CH ₃	0	C ₂₇ H ₃₃ N ₃ O ₄	3.02 × 10 ⁻⁹	8.52
17	C ₆ H ₁₁ ^{a)}	2	CH ₂ CH ₃	0	C ₂₈ H ₃₅ N ₃ O ₄	1.09 × 10 ⁻⁹	8.96
18	C ₆ H ₁₁ ^{a)}	3	CH ₃	0	C ₂₈ H ₃₅ N ₃ O ₄	3.52 × 10 ⁻⁹	8.45
19	C ₆ H ₁₁ ^{a)}	3	CH ₂ CH ₃	0	C ₂₉ H ₃₇ N ₃ O ₄	2.23 × 10 ⁻⁹	8.65
20	C ₆ H ₁₁ ^{a)}	4	CH ₃	0	C ₂₉ H ₃₇ N ₃ O ₄	4.94 × 10 ⁻⁹	8.30
21	C ₆ H ₁₁ ^{a)}	4	CH ₂ CH ₃	0	C ₃₀ H ₃₉ N ₃ O ₄	6.31 × 10 ⁻⁹	8.20
22	C ₆ H ₅	1	CH ₃	0	C ₂₆ H ₂₅ N ₃ O ₄	2.71 × 10 ⁻¹⁰	9.56
23	C ₆ H ₅	1	CH ₂ CH ₃	0	C ₂₇ H ₂₇ N ₃ O ₄	2.11 × 10 ⁻¹⁰	9.67
24*	C ₆ H ₅	2	CH ₃	0	C ₂₇ H ₂₇ N ₃ O ₄	5.23 × 10 ⁻¹⁰	9.28
25	C ₆ H ₅	2	CH ₂ CH ₃	0	C ₂₈ H ₂₉ N ₃ O ₄	1.90 × 10 ⁻¹⁰	9.72
26	4-CH ₃ -C ₆ H ₄	2	CH ₃	0	C ₂₈ H ₂₉ N ₃ O ₄	3.24 × 10 ⁻¹⁰	9.49
27	4-CH ₃ -C ₆ H ₄	2	CH ₂ CH ₃	0	C ₂₉ H ₃₁ N ₃ O ₄	5.75 × 10 ⁻¹⁰	9.24
28	C ₆ H ₅	3	CH ₃	0	C ₂₈ H ₂₉ N ₃ O ₄	5.84 × 10 ⁻¹⁰	9.23
29*	C ₆ H ₅	3	CH ₂ CH ₃	0	C ₂₉ H ₃₁ N ₃ O ₄	8.75 × 10 ⁻⁹	8.05
30	C ₆ H ₅	4	CH ₃	0	C ₂₉ H ₃₁ N ₃ O ₄	6.14 × 10 ⁻⁹	8.21
31	C ₆ H ₅	4	CH ₂ CH ₃	0	C ₃₀ H ₃₃ N ₃ O ₄	5.02 × 10 ⁻⁹	8.30

*Compounds used for external test set. Experimental activity values (IC₅₀) from ref. [6].
Index a: Cyclohexyl and index b: Cyclopentyl

During the year 2013, Hadizadeh et al. [22] developed an MLR model to discover new compounds, such as CCB, using descriptors calculated by DRAGON software.

Da Mota et al. [23] proposed two analogues with activities comparable to known calcium channel blockers after using several methods namely: MIA-QSAR, docking and drug-like. Additionally Jardinez et al. [24] applied the reduced density gradient approach to calculate QSAR descriptors, on 1,4-dihydropyridine derivatives such as antihypertensives

Recently, El-Moselhy et al. [25] constructed 3D-QSAR models; these approaches are based on synthesized molecules and with inspiration from molecular docking investigations.

In this study, the investigated molecules, containing 4-imidazolyl substituents, were synthesized by Navidpour et al. [26]. Two statistical methods namely multiple MLR and ANN were used for the development of QSAR models (QSAR/MLR and QSAR/ANN). We also used the DFT quantum method for geometric optimization of structures and calculations of quantum descriptors.

2. Computational Method

2.1. Dataset

A series of 31 compounds, known as DHP14, were examined in a previous publication for their

biological activity and revealed good activity as calcium channel blockers (CCBs) [26]. These compounds share the same core structure, DHP14, and are substituted by ester systems in positions 3 and 5 in addition to a phenyl imidazolyl group. Their biological activity as CCBs was influenced by these structural alterations as displayed in Table 1. To clarify these structural alterations and their role in biological activity, these compounds were retrieved for further study. All of the compounds that were examined are shown simultaneously in Table 1 and Scheme 1.

2.2. Drug likeness

The drug likeness descriptors of the investigated were in silico predicted using HyperChem 8.03 [27], and Molinspiration via the site (<http://www.molinspiration.com>). These descriptors including molecular weight (MW), topological polar surface area (TPSA), number of rotatable bonds (Nrotb), molar refractivity (MR), hydrogen bond donors (HBD), and hydrogen bond acceptors (HBA) are known to be closely associated with key molecular properties such as solubility, bioavailability, and permeability through membranes [28].

Lipinski's Rule states that compounds that have less than 500 Da of molecular weight, less than 5 log P values (lipophilicity), less than 5 hydrogen bond

Siham Aggoun, Salah Belaidi, Lazhar Bouchlaleg, Hassan Nour, Oussama Abchir, Samir Chtita, Muneerah Mogren Almogren, Majdi Hochlaf

donors, and less than 10 hydrogen bond acceptors will probably be better absorbed when taken orally [29]. Additionally, Veber's rule states that compounds having a total polar surface area (TPSA) of less than 140 \AA^2 and fewer than 10 rotatable bonds are more likely to have good bioavailability [30].

Furthermore, according to Ghose's rule [31], substances having a total number of atoms between 20 and 70, a molecular weight between 160 and 480 Da, a log P value between -0.4 and 5.6, and a molar refractivity (MR) between 40 and 130 are thought to have advantageous drug-like qualities.

2.3. Molecular docking analysis

Molecular docking investigations [32-33] were performed using Autodock Vina software [34] to determine the mode of interaction of the DHP14 derivatives and the target receptor (Calcium Channels).

The crystal structure of Calcium Channel, was taken from the Protein Data Bank (PDB ID: 5KMD). After removing all bound ligands from the target, the polar hydrogens were added, and Kollman charges were calculated using AutoDock4 tools. The grid box was set as: ($x = 39.626 \text{ \AA}$, $y = 36.709 \text{ \AA}$, $z = 14.846 \text{ \AA}$) at 20 \AA size with a spacing of 0.375 \AA . While the geometries of the ligand structures have been optimized with the mathematical algorithm of the steepest descent with the Avogadro program [35]. Finally, the DHPs were docked to CCBs and the ligand-receptor interactions were analyzed and interpreted by using the Discovery Studio program 2021 [36].

2.4. Investigated structures and electronic descriptors.

The structures of the DHP14 derivatives have been optimized using the Gaussian 16 software [37] and to estimate their quantum descriptors using the DFT method, at B3LYP/6-31G+(d,p) level [37]. The DFT method has been widely used in recent years, particularly in our previous work [38-42]. The HOMO and LUMO orbitals are called frontier orbitals, which are major parameters in quantum chemistry because they determine how the molecule reacts with neighboring chemical entities. The value of the frontier orbital gap allows us to estimate and characterize the kinetic stability and the chemical reactivity of the studied molecule ($E_{\text{gap}} = E_{\text{LUMO}} - E_{\text{HOMO}}$). A molecule which has a small

gap is more polarizable, that is to say associated with a strong reactivity and a weak kinetic stability and it is called a soft molecule, The conceptual descriptors based on the DFT quantum method have facilitated a good understanding of the 3D structure of biomolecules and their reactivity by computational calculation of the global hardness (η) and the chemical potential (μ). These two potentials are calculated according to the frontier orbitals as follows: the chemical potential μ is equal to $(E_{\text{HOMO}} + E_{\text{LUMO}})/2$ and the global hardness is given by $\eta = (-E_{\text{HOMO}} + E_{\text{LUMO}})/2$ [43]. This index assesses the stability of the molecule when the electronic system has received an additional charge from its vicinity. Electrophilia therefore has a double capacity, the first to gain an electronic charge and the second to resist an exchange of electronic charge with its surroundings. The overall electrophilic power (ω) of a biomolecule (ligand) is given by the following relationship: $\omega = \mu^2/2\eta$.

2.5. QSAR analysis

The construction of a QSAR model is carried out by three essential stages: The first step is the preparation of the data, the second is the analysis of the data and finally the last is the validation of the model. The resulting models are then used to select new ligands based on the results obtained and the predicted biological activities in order to find a model that has a very predictive power.

In this work we used two different methods of chemoinformatics techniques, the first one is Multiple Linear Regression (MLR) method and the second method is Artificial Neural Networks (ANN), were used to correlate the relationship between the biological activity of ligands and corresponding descriptors.

For the construction of the model, we randomly divided the collected series in two sets; a training and a test set. We calculated the internal validation indices and the parameters of external validation to test the reliability and the quality of our built models, as well as the y-randomization test parameters to have an overview of the robustness of the model, in which. We have identified the domain of applicability of the model to be used as a tester to discover novel ligands with improved CCB activities.

Siham Aggoun, Salah Belaidi, Lazhar Bouchlaleg, Hassan Nour, Oussama Abchir, Samir Chtuta, Muneerah Mogren Almogren, Majdi Hochlaf

3. Results and discussion

3.1. Drug likeness evaluation

All compounds were subjected to the drug likeness assessment using Hyperchem software, and moolinspiration site. The results were listed in Table 2 and showed that except for ligands 22, 23, 24 and 26, all compounds have a value of the partition coefficient (LogP) ranging between 0 and 5, which results in good oral bioavailability; ie has good aqueous solubility to dissolve in gastrointestinal fluids and good permeability to cross biological membranes. A negative value for log P, ($\text{LogP} < 0, P < 1$), which has the consequence that the ligand is too hydrophilic, so it has better water solubility and easy renal elimination, but low permeability and poor binding to plasma proteins. A positive value for log P, ($\text{LogP} > 0 P > 1$), it has the consequence that the ligand is too lipophilic, therefore it has good permeability through the membrane, better binding to blood plasma proteins and metabolic elimination by the liver, but low solubility in aqueous media and difficult gastric tolerance [44].

Molecular weight (MW) is a major factor influencing drug permeability, for molecules with

molar mass < 450 , it results in better cerebral permeability and through lipid bilayer membranes this is the case for ligands 12, 13, 14 and 22 [45].

All the ligands have values of HBA (H-bond acceptors) lower than 10 and HBD (H-bond donors) lower than 5, so they respect Lipinski's rule well. high number of HBA results in poor permeability through lipophilic biological barriers, while lower number result in good permeability [46,47].

The topological polar surface area (TPSA) is a primary factor in predicting the intrinsic properties of ligand transport in the body, especially in permeability, that is to say the speed of passage of molecules through the blood-brain barrier and also in intestinal absorption [48]. By a simple reading of the results, we see that all the ligands have values lower than 140 \AA^2 , so it respects Veber's rule well, which compares the oral bioavailability of the ligand to molecular flexibility.

In conclusion, the majority of the ligands respect the rules of Lipinski, Veber and Ghose. In the particular case, ligand 12 has the best scoring in the three rules mentioned above. So these rules help us select the lead compound.

Table 2. Properties of DHP14 and rules scoring.

Compound	Molecular Weight (amu)	Log P	HBD	HBA	Lipinski Score	Number Rotatable Bonds	TPSA	Veber Score	N atoms	MR	Ghose Score
(1)	503.28	1.64	2	7	3	8	93.32	2	37	150.09	2
(2)	531.31	2.27	2	7	3	10	93.32	2	39	159.55	2
(3)	559.34	2.91	2	7	3	12	93.32	1	41	168.91	2
(4)	587.37	3.71	2	7	3	14	93.32	1	43	178.11	2
(5)	615.40	4.50	2	7	3	16	93.32	1	45	187.31	2
(6)	559.34	2.91	2	7	3	14	93.32	1	41	168.91	2
(7)	519.22	0.50	2	7	3	10	93.32	2	39	165.57	2
(8)	547.25	1.00	2	7	3	12	93.32	1	41	175.08	2
(9)	575.28	1.79	2	7	3	14	93.32	1	43	184.28	2
(10)	603.31	2.58	2	7	3	16	93.32	1	45	193.48	2
(11)	631.34	3.38	2	7	3	18	93.32	1	47	202.68	2
(12)	435.22	0.05	2	7	4	7	93.32	2	32	129.08	4

Siham Aggoun, Salah Belaidi, Lazhar Bouchlaleg, Hassan Nour, Oussama Abchir, Samir Chtuta, Muneerah Mogren Almogren, Majdi Hochlaf

(13)	449.23	0.40	2	7	4	8	93.32	2	33	133.82	3
(14)	449.23	0.37	2	7	4	8	93.32	2	33	133.81	3
(15)	463.25	0.71	2	7	4	9	93.32	2	34	138.56	3
(16)	463.25	0.69	2	7	4	9	93.32	2	34	138.49	3
(17)	477.26	1.03	2	7	4	10	93.32	2	35	143.23	3
(18)	477.26	1.09	2	7	4	10	93.32	2	35	143.09	3
(19)	491.28	1.43	2	7	4	11	93.32	1	36	147.84	2
(20)	491.28	1.48	2	7	4	11	93.32	1	36	147.69	2
(21)	505.29	1.83	2	7	3	12	93.32	1	37	152.44	2
(22)	443.18	-0.52	2	7	4	8	93.32	2	33	136.81	3
(23)	457.20	-0.17	2	7	4	9	93.32	2	34	141.56	3
(24)	457.20	-0.27	2	7	4	9	93.32	2	34	141.57	3
(25)	471.22	0.08	2	7	4	10	93.32	2	35	146.32	3
(26)	471.22	-0.11	2	7	4	9	93.32	2	35	145.85	3
(27)	485.23	0.23	2	7	4	10	93.32	2	36	150.60	2
(28)	471.22	0.13	2	7	4	10	93.32	2	35	146.17	3
(29)	485.23	0.47	2	7	4	11	93.32	1	36	150.92	2
(30)	485.23	0.53	2	7	4	11	93.32	1	36	150.77	2
(31)	499.25	0.87	2	7	4	12	93.32	1	37	155.52	2

Table 3. Binding energies of the complexes.

Compounds	Binding Energy (kcal/mol)	Compounds	Binding Energy (kcal/mol)
1	-8.3	17	-8.3
2	-7.9	18	-7.8
3	-7.8	19	-7.9
4	-8.7	20	-8.1
5	-6.9	21	-7.6
6	-8.4	22	-7.9
7	-7.7	23	-7.7
8	-8.3	24	-8.5
9	-9.0	25	-8.2
10	-7.2	26	-8.8
11	-7.4	27	-8.4
12	-8.0	28	-8.7
13	-7.8	29	-8.5
14	-8.1	30	-8.4
15	-7.8	31	-8.1
16	-7.9	Amlodipine	-5.5

Siham Aggoun, Salah Belaidi, Lazhar Bouchlaleg, Hassan Nour, Oussama Abchir, Samir Chtuta, Muneerah Mogren Almogren, Majdi Hochlaf

3.2. Molecular docking.

The molecular docking of all studied compounds in the binding site of target was performed using Autodock software, the Amlodipine was also docked as the reference drug to compare the obtained results. the binding energy were listed in Table 3, and good values of binding energy was observed for all created complexes, it may due to the type, and the number of the formed interactions between the ligands and the main residues of target. We note that all ligands have lower binding energies compared to the reference drug amlodipine.

Initially, we looked at the interactions between the drug Amlodipine and the calcium channel target.

The key residues that characterize the active site of the receptor have been identified through the analysis of the active sites of Amlodipine. Figure 2 shows that amlodipine binds to the receptor, with the involvement of three hydrogen bonds with (GLY D): 1164, and two π - π interactions with (PHE D): 1167 and (TYR C): 1195. It can be deduced that these three hydrogen bonds are considered to be the most powerful key residues, thus influencing the activity of calcium channels. The multiple interactions between the most active ligands: 2, 3 and 4 and their target have been interpreted and analyzed; to understand their high IC_{50} values.

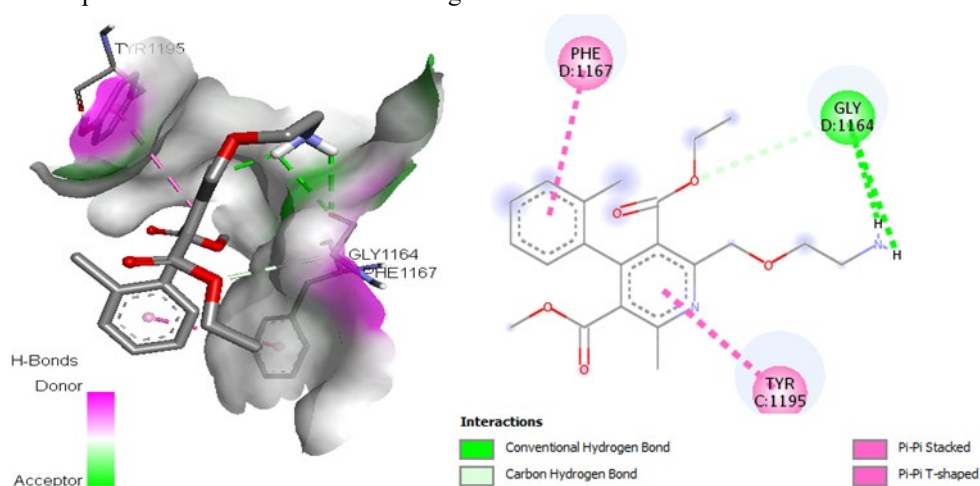
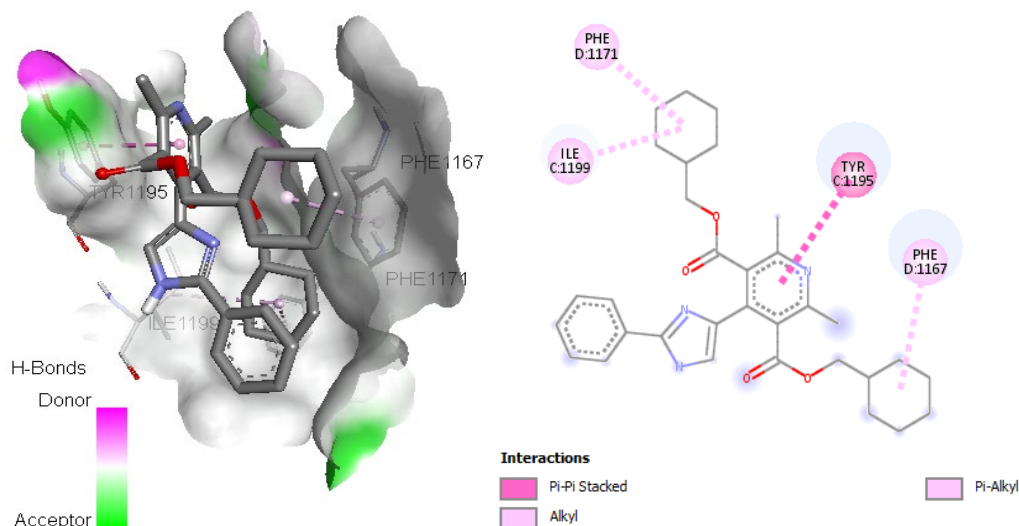


Figure 2. 2D and 3D interactions between amlodipine and the calcium channel target.



Siham Aggoun, Salah Belaidi, Lazhar Bouchlaleg, Hassan Nour, Oussama Abchir, Samir Chtuta, Muneerah Mogren Almogren, Majdi Hochlaf

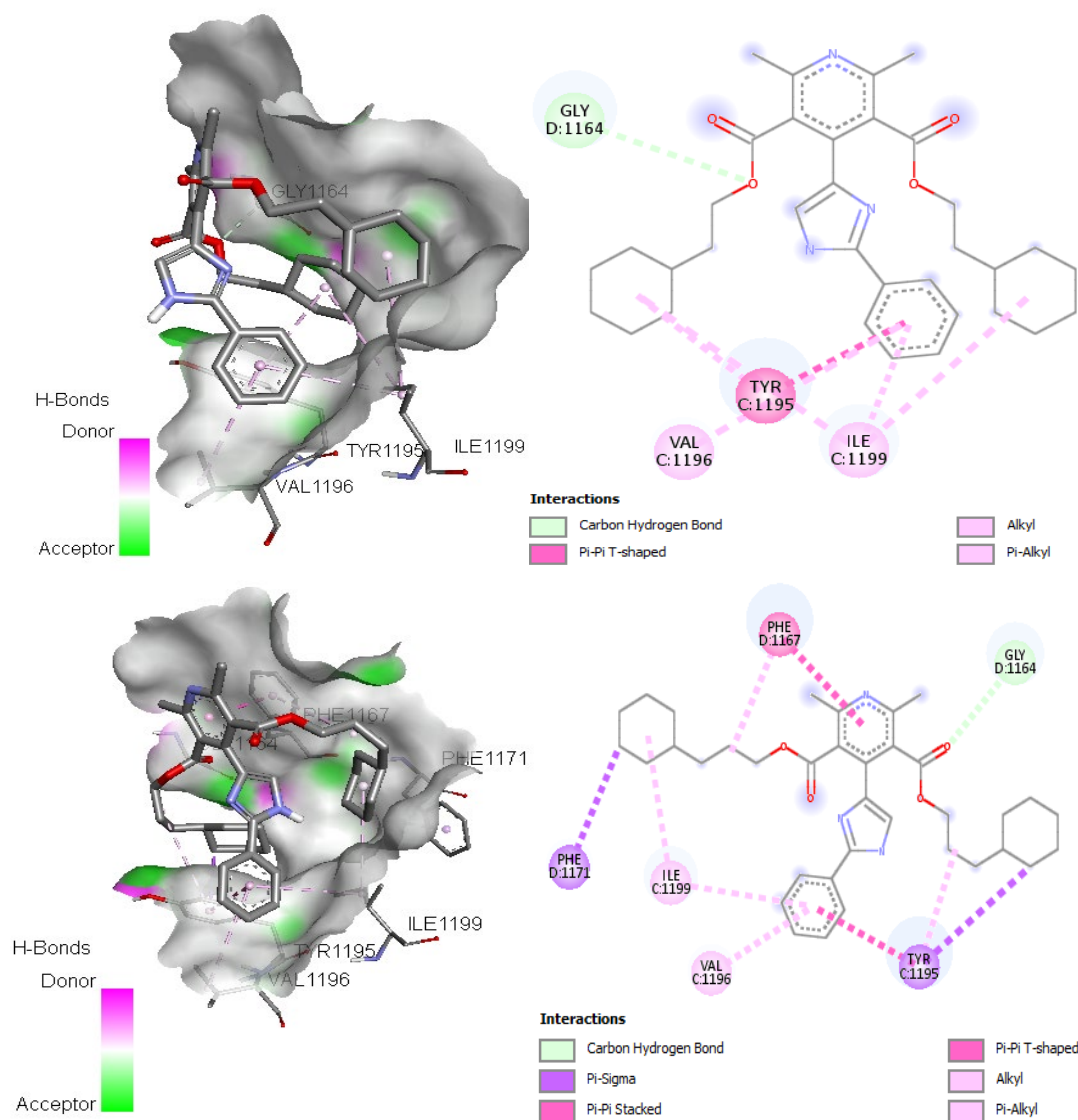


Figure 3. 2D and 3D interactions between the calcium channel crystal structure and the compounds (2:Top, 3: Middle and 4: Bottom).

Table 5. The predicted molecular descriptors for the 29 studied compounds.

N	EM	LogS	NRB	SC	SVD	TD	MR	HE	V	SAG	logP	E _{HOMO}	E _{LUMO}	E _{HOMO-1}	E _{LUMO+1}	D	E	η	χ	E _{Gap}
1	503.28	-7.50	8	1	122	14	150.09	-4.21	1451.63	812.16	1.64	-5.24	-1.63	-5.83	-0.47	3.92	-44361.11	1.81	3.44	3.61
2	531.31	-8.40	10	1	126	16	159.55	-3.62	1569.04	870.21	2.27	-5.28	-1.68	-5.88	-0.51	3.75	-46499.93	1.80	3.48	3.60
3	559.34	-8.78	12	1	130	18	168.91	-2.24	1756.62	1003.51	2.91	-5.26	-1.65	-5.85	-0.49	3.81	-48639.02	1.80	3.46	3.61
4	587.37	-9.46	14	1	134	20	178.11	-3.07	1846.21	1052.63	3.71	-5.26	-1.66	-5.86	-0.50	3.73	-50778.11	1.80	3.46	3.60
5	615.40	-10.14	16	1	138	22	187.31	-1.01	1988.95	1150.05	4.50	-5.26	-1.66	-5.86	-0.50	3.77	-52916.92	1.80	3.46	3.61
6	559.34	-8.67	14	1	130	18	168.91	-2.96	1713.28	979.85	2.91	-5.26	-1.66	-5.87	-0.50	3.73	-48638.47	1.80	3.46	3.60
7	519.22	-7.80	10	1	138	16	165.57	-10.4	1448.30	814.67	0.50	-5.21	-1.71	-5.89	-0.57	4.08	-46302.92	1.75	3.46	3.50
8	547.25	-8.09	12	1	142	18	175.08	-9.61	1599.33	915.66	1.00	-5.31	-1.72	-5.92	-0.55	3.79	-48442.01	1.80	3.52	3.59
9	575.28	-8.63	14	1	146	20	184.28	-8.88	1684.03	954.11	1.79	-5.28	-1.70	-5.89	-0.51	3.70	-50580.82	1.79	3.49	3.59
10	603.31	-9.47	16	1	150	22	193.48	-8.21	1793.49	1008.54	2.58	-5.30	-1.70	-5.90	-0.53	3.74	-52719.91	1.80	3.50	3.60
11	631.34	-10.31	18	1	154	24	202.68	-7.66	1880.58	1063.00	3.38	-5.28	-1.69	-5.89	-0.51	3.74	-54859.00	1.79	3.48	3.59
12	435.22	-5.79	7	1	110	14	129.08	-5.39	1252.30	713.83	0.05	-5.28	-1.68	-5.87	-0.49	4.12	-39046.18	1.80	3.48	3.60
13	449.23	-6.13	8	1	112	14	133.82	-4.81	1308.63	745.27	0.40	-5.27	-1.66	-5.85	-0.49	4.08	-40115.86	1.81	3.46	3.62
14	449.23	-6.24	8	0	112	15	133.81	-5.02	1324.04	761.86	0.37	-5.28	-1.70	-5.90	-0.52	3.77	-40115.59	1.79	3.49	3.58
15	463.25	-6.58	9	0	114	15	138.56	-4.41	1376.32	793.15	0.71	-5.28	-1.68	-5.88	-0.51	3.77	-41185.27	1.80	3.48	3.60
16	463.25	-6.81	9	1	114	16	138.49	-4.43	1447.98	825.77	0.69	-5.27	-1.69	-5.89	-0.50	3.97	-41185.00	1.79	3.48	3.58
17	477.26	-7.15	10	1	116	16	143.23	-3.85	1483.56	854.08	1.03	-5.26	-1.67	-5.87	-0.50	3.91	-42254.68	1.80	3.47	3.60
18	477.26	-7.22	10	0	116	17	143.09	-4.40	1462.37	844.40	1.09	-5.27	-1.69	-5.89	-0.51	3.79	-42254.41	1.79	3.48	3.58
19	491.28	-7.56	11	0	118	17	147.84	-3.88	1524.98	886.22	1.43	-5.27	-1.67	-5.87	-0.50	3.86	-43324.09	1.80	3.47	3.60

Siham Aggoun, Salah Belaidi, Lazhar Bouchlaleg, Hassan Nour, Oussama Abchir, Samir Chtuta, Muncerah Mogren Almogren, Majdi Hochlaf

20	491.28	-7.64	11	1	118	18	147.69	-3.78	1511.14	880.51	1.48	-5.27	-1.69	-5.90	-0.51	3.89	-43324.09	1.79	3.48	3.58
21	505.29	-7.98	12	1	120	18	152.44	-3.29	1562.52	899.07	1.83	-5.27	-1.67	-5.87	-0.50	3.83	-44393.77	1.80	3.47	3.60
22	443.18	-5.93	8	0	118	15	136.81	-8.27	1262.50	723.19	-0.52	-5.22	-1.70	-5.89	-0.57	3.76	-40016.81	1.76	3.46	3.51
23	457.20	-6.27	9	0	120	15	141.56	-7.69	1318.10	552.38	-0.17	-5.22	-1.68	-5.87	-0.57	3.71	-41086.49	1.77	3.45	3.54
24	457.20	-6.08	9	1	120	16	141.57	-8.15	1336.03	772.92	-0.27	-5.30	-1.72	-5.92	-0.54	3.92	-41086.49	1.79	3.51	3.58
25	471.22	-6.42	10	1	122	16	146.32	-7.57	1389.85	801.39	0.08	-5.30	-1.70	-5.90	-0.53	3.84	-42156.17	1.80	3.50	3.59
26	471.22	-6.44	9	0	122	17	145.85	-6.95	1381.48	801.95	-0.11	-5.19	-1.70	-5.89	-0.48	3.61	-42156.17	1.75	3.44	3.49
27	485.23	-6.78	10	0	124	17	150.60	-6.38	1436.92	829.38	0.23	-5.19	-1.68	-5.87	-0.47	3.56	-43225.85	1.76	3.43	3.51
28	471.22	-6.35	10	0	122	17	146.17	-7.72	1381.76	799.42	0.13	-5.28	-1.71	-5.91	-0.52	3.78	-42155.90	1.79	3.50	3.57
29	485.23	-6.69	11	0	124	17	150.92	-7.14	1436.81	831.57	0.47	-5.28	-1.69	-5.89	-0.51	3.73	-43225.58	1.80	3.49	3.59
30	485.23	-6.77	11	1	124	18	150.77	-7.42	1491.96	873.56	0.53	-5.29	-1.71	-5.92	-0.53	3.78	-43225.58	1.79	3.50	3.58
31	499.25	-7.11	12	1	126	18	155.52	-6.84	1547.91	903.90	0.87	-5.29	-1.69	-5.90	-0.53	3.73	-44295.26	1.80	3.49	3.60

Notes: Exact Mass(EM)// Intrinsic Solubility (Log S)// Number of Rotatable Bonds(NRB)// Shape Coefficient(SC)// Sum of Valence Degrees(SVD)// Topological Diameter(TD)// Molar Refractivity(MR)// Hydration Energy(HE)// Molar Volume(V)// Surface Area Grid(SAG)// logarithm of the partition Coefficient(Log P)// Dipole moment (Debye)// Total energy: E (eV)// Hardness:η(eV)// Electronegativity: χ(eV)// Energy Gap :E_{Gap}(eV) //molecular orbitals: E_{HOMO}, E_{LUMO}, E_{HOMO-1} and E_{LUMO+1} in(eV).

Figure 3 shows that ligand 2 mainly interacts with two key residues, namely (TYR C):1195, (PHE D):1167 via a π - π interaction with (TYR C):119 as well as a π -alkyl interaction with (PHE D): 1167 in addition to other interactions with (PHE D): 1171 and (ILE C): 1199, which justifies its potency as a calcium channel blocker.

In addition, compound 3 is complexed with the target, this complex involves five alkyl interactions with (ILE C): 1199, (TYR C): 1195 and (VAL C): 1196 a π - π interaction with (TYR C): 1195 and a hydrogen bond with (GLY D): 1164. The amino acids TYR C and GLY, which the ligand 3 interacts, are active sites which influence the biological activity of the Calcium Channel receptor, this well justifies the activity observed from this ligand to the target.

Ligand 4 is the most active of all studied compounds, it interacts with all the key residues which have an influence on the activity of the CCB. Furthermore, this ligand is linked in a hydrogen bond with (GLY D): 1164, four alkyl interactions with (TYR C): 1195, (PHE D): 1167, (ILE C): 1199 and (VAL C): 1196, two two π - π interactions with (PHE D): 1167 and (TYR C): 1195, and finally two π - π with (TYR C): 1195 and (PHE D): 1171.

The comparison of the number of interactions in the complexes, between the key residues and the most active ligands. (Table 4), gives us a rigorous interpretation of the good biological activity against CCB, this is also well demonstrated by experience. We find that we have more efficient activity if the number of interactions of the ligands with the key residues is high. Thus, according to the results of docking, they validate and verify the activities observed (in vitro) for the DHP14 derivatives studied [26].

Table 4. Interactions between key residues and the most active ligands.

Compound	pIC ₅₀	Interacting sites		
		GLY D	PHE D	TYR C
2	10.44	0	1	1
3	10.74	1	0	2
4	10.92	1	2	3

3.3. DFT study

Based on our previous works, as in the following references [38-42], the common subunit analysis of all ligands can help to understand their 3D structure and the structural components that well influence their CCBs activities. We noticed that the 3D conformation of 4-imidazolyl-1,4-dihydropyridine, which is the basic structure of DHP14's, changes its 3D conformation after the introduction of the different substituents.

According to Figure 4, Compound 3 has a conformation composed of two parallel planar systems: phenyl and imidazolyl, while the DHP14 moiety is nearly orthogonal to both systems. In the series of ligands studied, three cycles are however close to the plane, which favors their stabilization by a delocalization of the electronic system on these three cycles. The differences in conformation between the basic structure (single subunit) and the different ligands are interpreted by the presence of more long-lasting interactions between the phenyl substituents and the alkoxy substituents attached to the esters.

3.4. QSAR studies

Several molecular descriptors were calculated for each compound of the studied 29 compounds by using Dragon, and Gaussian 16 programs. These

Siham Aggoun, Salah Belaidi, Lazhar Bouchlaleg, Hassan Nour, Oussama Abchir, Samir Chtuta, Muneerah Mogren Almogren, Majdi Hochlaf

descriptors were collected to form a dataset with the corresponding biological activity to predict which among influence the CCB activity. among these descriptors the octanol/water partition coefficient/Log P, the intrinsic solubility/Log S, the exact mass /EM, the number of rotatable bonds/NRB, the sum of the degrees of valence/SVD, the shape coefficient/SC, the topological diameter/TD, the energy of hydration/HE, the molar efractivity /MR, the molar volume/ V and the surface grid/SAG. Table 5 presents the calculated molecular descriptors (Quantum, and non-quantum descriptors) with their corresponding biological activity[49-51].

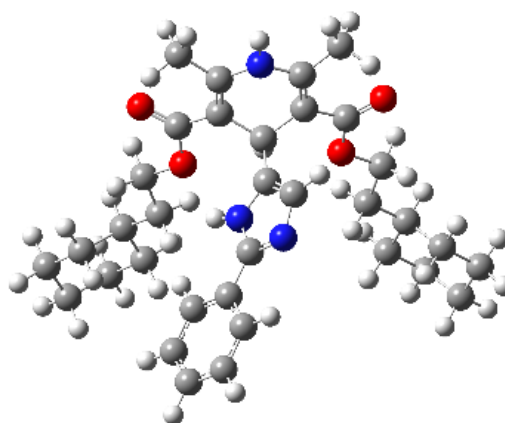


Figure 4. The optimized conformation of the Compound 3.

QSAR models try to correlate a numerical value of the molecular structure to an observable entity such as biological activity or a chemical property, for example the retention index. In general, the QSAR equations relate an activity or a physical-chemical property of an observable and measurable type to a certain selected descriptors whose number is well defined beforehand.

In this work, the statistical software under Excel: XLSTAT software [52] is used for multiple linear regression (MLR) and the numerical calculation

platform: Matlab tools [53] for investigations on artificial neural networks (ANNs).

3.4.1. MLR Regression Application

Multiple linear regression (MLR) is the most used molecular modeling method, it is the extension of simple linear regression to the multivariate cas. The objective of the MLR statistical method is to correlate the linear relationship between the independent variables and the dependent response variable [54].

In this study, a reliable correlation was found between the activity of Calcium Channel Blocker and the calculated descriptors which is given by the following equation of mathematical model:

$$(\text{pIC}_{50}) = 4.089 + 1.871 \text{ Log S} - 1.242 \text{ NRB} - 0.494 \text{ SVD} + 0.568 \text{ MR} - 12.480 \text{ E}_{\text{LUMO}+1}$$

According to the correlation equation, we find that Calcium Channel Blocker activity is a function of the following decriptors which directly influences the activity: the intrinsic solubility, the number of rotatable bonds, the sum of the degrees of valence, molar refractivity and energy of LUMO⁺¹. We also note that the following coefficients of the mathematical model equation: Log S and MR are positive, while the rest of the coefficients are negative. Therefore, if one increases the values of the descriptors of log S and MR or decreases the values of NRB, SVD and E_{LUMO+1}, it improves the CCB activity.

The activities predicted by the QSAR/MLR mathematical model are shown in Table 6. Figure 5 presents the graph of the values of the activities predicted as a function of the experimental values. We noticed that the values of the predicted CCB activities are in good agreement with the values derived from the experiment, with the coefficient of determination $R^2_{\text{test}} = 0.684$ for the test set and $R^2 = 0.762$ for the learning set, this shows the good correlation between the variables with the desired activity.

Table 6. Experimental and Predicted pIC₅₀ using MLR, and ANN models.

(N°)	(Exp)	(Pred.)		(N°)	(Exp.)	(Pred.)	
		MLR	ANN			MLR	ANN
(1*)	9.52	10.93	10.93	16	8.52	8.81	8.97
(2)	10.44	10.75	10.35	17	8.96	8.59	8.68
(3)	10.74	10.64	10.69	18	8.45	8.48	8.74
(4)	10.92	10.21	10.43	19	8.65	8.24	8.42
(5)	9.19	9.68	9.45	20	8.30	8.08	8.48

Siham Aggoun, Salah Belaidi, Lazhar Bouchlaleg, Hassan Nour, Oussama Abchir, Samir Chtita, Muneerah Mogren Almogren, Majdi Hochlaf

(6)	8.55	8.41	8.90	21	8.20	7.86	8.15
(7 [*])	9.25	10.01	10.01	22	9.56	9.56	9.37
(8 [*])	9.34	10.17	10.17	23	9.67	9.46	9.19
(9)	10.01	9.50	10.09	24[*]	9.28	9.38	9.38
(10)	9.19	8.98	8.92	25	9.72	9.16	8.72
(11)	7.05	7.90	8.11	26	9.49	9.44	9.41
(12)	9.75	9.65	9.25	27	9.24	9.18	9.35
(13)	9.07	9.45	9.02	28	9.23	9.02	8.62
(14)	8.55	9.59	9.13	29[*]	8.05	8.79	8.79
(15 [*])	8.88	9.35	9.35	30	8.21	8.77	8.34
				31	8.30	8.55	7.92

(* denotes: compounds selected for test set).

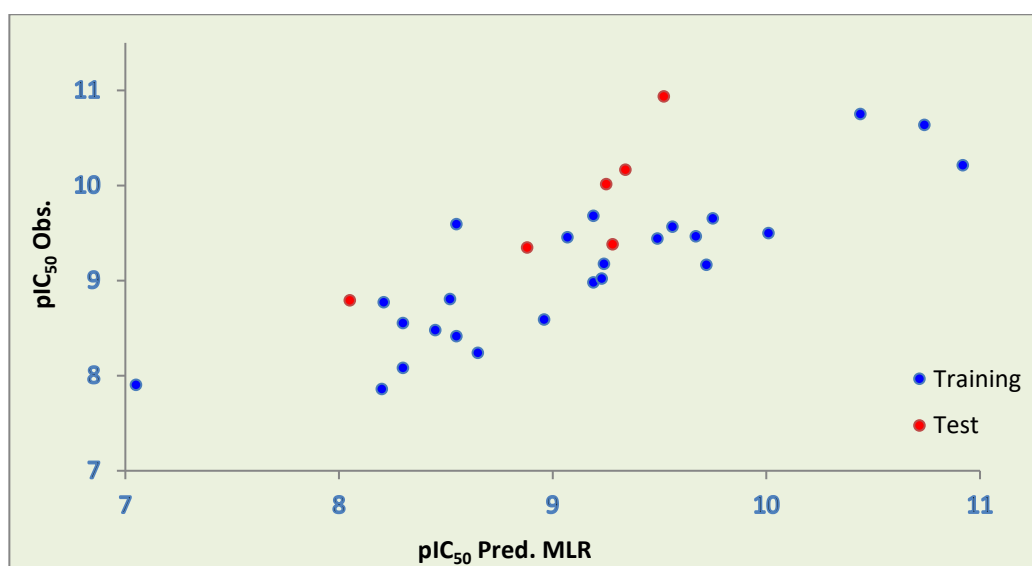


Figure 5. Correlation between experimental and predicted pIC_{50} values.

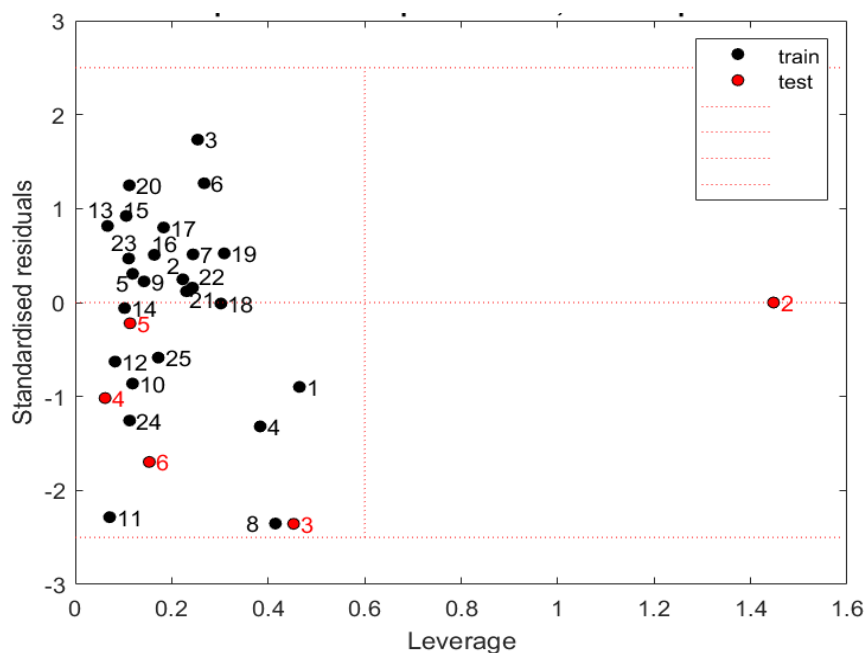


Figure 6. William's plot of QSAR/MLR model.

1-Residual bounds ± 2.5 and $h^* = 0.250$ 1-The dotted red lines show the interval that delimits the domain of applicability. 2- Test samples are in red dots and training samples are in black dots.

Siham Aggoun, Salah Belaidi, Lazhar Bouchlaleg, Hassan Nour, Oussama Abchir, Samir Chtita, Muneerah Mogren Almogren, Majdi Hochlaf

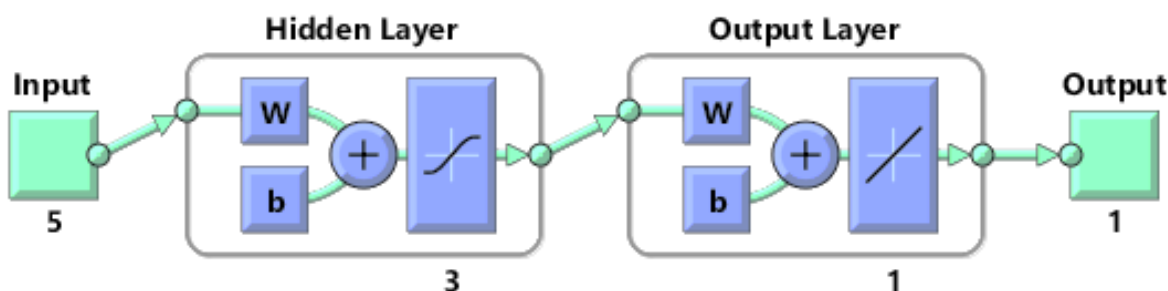


Figure 7. ANN Structure.

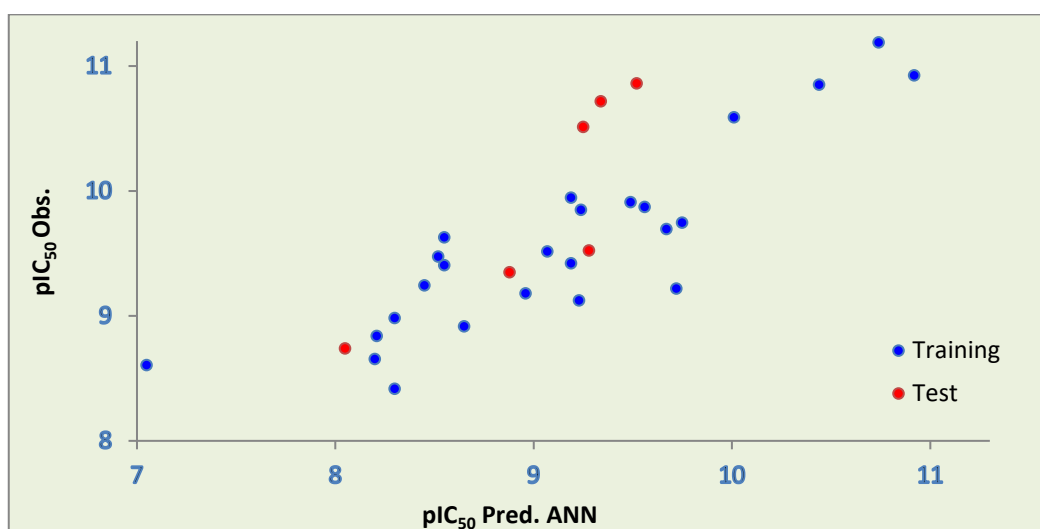


Figure 8. Correlation of predicted and experimental pIC50 values validated by the ANN model.

The structure of ANN is presented by a neural network which is a complex system composed of neurons interconnected and divided into three layers. From Figure 7, input layer is composed of five neurons, each neuron receiving one of the five descriptors in the QSAR/MLR model (Log S, NRB, SVD, MR and E_{LUMO+1}). The most important layer is the hidden layer also known by the word middle contains three neurons which form the deep internal entity which reveals the most interesting relationship between experimental values and predicted values. The output layer is represented by a neuron, which takes care of sending back the value of pIC₅₀ [62], and in Table 6 we find the values of the predicted activities, calculated by the ANN model. Figure 8 presents the predicted activities as a function of the experimental activities using the QSAR/ANN modeling. Therefore the values of the predicted CCB activities are in good agreement with the values drawn from the experiment. This shows us a robust relationship between the five descriptors with calcium channel blocker activity. Robustness and reliability of the

QSAR/ANN modeling was validated and confirmed by the following parameters: a correlation coefficient of ($R^2 = 0.767$), and the test data set ($R^2_{test} = 0.876$).

4. Conclusions

The QSAR/MLR and QSAR/ANN analysis were conducted with a series of DHP14 derivatives as the Calcium Channel Blockers. The reliability and robustness of the models designed was validated using internal and external statistical validation techniques to justify the prediction quality of these models. These QSAR/MLR and QSAR/ANN models are well supported by external validation, thus proving their powers to predict with remarkable accuracy the Calcium Channel Blocker activity of the ligands in the series. According to the correlation equation of the QSAR/MLR model, we found that the Calcium Channel Blocker activity is a function of following descriptors which directly influence the activity: number of rotatable bonds, intrinsic solubility, the sum of the degrees of valence, molar refractivity and energy of LUMO+1.

Siham Aggoun, Salah Belaidi, Lazhar Bouchlaleg, Hassan Nour, Oussama Abchir, Samir Chtita, Muneerah Mogren Almogren, Majdi Hochlaf

It can be noticed that the values of predicted BCC activities are in good agreement with the experimental values with correlation coefficient $R^2_{\text{test}} = 0.684$ for test set and $R^2 = 0.762$ and for the training set, this shows a better correlation between the various variables. According to the QSAR/ANN model, the predicted CCB activity are in good agreement with those drawn from the experiment. The robustness and reliability of the QSAR/ANN model was justified and confirmed by the following parameters: a correlation coefficient ($R^2 = 0.767$) and test data set ($R^2_{\text{test}} = 0.876$). The majority of ligands respect Dri-like filters: Lipinski, Ghose and Veber. In the particular case, ligand 12 has the best scoring in the three rules mentioned above. So these rules help us select Lead compounds. The docking approach guided us to explain the mechanism of the interactions inside the complexes between the CCB activity and this type of bioactive ligands. Concerning ligand 4, which is the most active among all the compounds studied, it interacts with all the key residues which have an influence on the activity of the CCB.

The good activity of the ligands against the CCB is deduced by the comparison of the number of interactions in the complexes, between the key residues and the most active ligands, as shown by the activities observed in vitro. We also find that we have more efficient activity if the interactions with key residues are varied and high, so they verify and substantiate the activities observed for the DHP14 derivatives studied.

ACKNOWLEDGMENTS

All authors thank the researchers for their contributions which supported by project number (RSPD2024R808) from King Saud University, Saudi Arabia.

References

- [1] A. Hantzsch, Condensation products made of aldehydammoniak and keton-like connections, *Chem. Ber.* 14, (1881) 1637-1638.
- [2] E. EisnerE, J. Kuthan, Chemistry of dihydropyridines, *Chem. Rev.* 72, (1972) 1-42.
- [3] D.J. Triggle, 1,4-Dihydropyridines as calcium channel ligands and privileged structures, *Cell. Mol. Neurobiol* 23, (2003) 293-303.
- [4] N. Edraki, A.R. Mehdipour, M. Khoshneviszadeh, R. Miri, Dihydropyridines: evaluation of their current and future pharmacological applications, *Drug Discov. Today* 14 (2009) 1058-66.
- [5] F. Bossert, W. Vater, 1,4-Dihydropyridines-a basis for developing new drugs, *Med. Res. Rev.* 9 (1989) 291-324.
- [6] F. Bossert, W. Vater, Dihydropyridine, eine neue Gruppe stark wirksamer Coronartherapeutika [Dihydropyridines, a new group of strongly effective coronary therapeutic agents], *Natur wissenschaften* 58 (1971) 578.
- [7] M. Epstein, H.R. Black, Arterial Calcification and Calcium Antagonists, *Hypertension* 37 (2001) 1414-1415.
- [8] V. Klusa, A typical 1,4-dihydropyridine derivatives, an approach to neuroprotection and memory enhancement, *Pharmacol. Res.* 113 (2016) 754-759.
- [9] V.K. Sharma, S.K. Singh, Synthesis, utility and medicinal importance of 1,2- & 1,4-dihydropyridines, *RSC Adv.* 7 (2017) 2682-2732.
- [10] C.A. Frank, J.M. Forst, R.J. Harris, S.T.Kau, J.H. Li, C.J. Ohmmachb, R.W. Smith, D.A.Trainor, S.Trivedi, Dihydropyridine KATP potassium channel openers, *Bioorg. Med. Chem. Lett.* 3 (1993) 2725-2726.
- [11] R.H.Bocker, F.P. Guengerich, Oxidation of 4-aryl- and 4-alkyl-substituted 2,6-dimethyl-3,5-bis(alkoxycarbonyl)-1,4-dihydropyridines by human liver microsomes and immunochemical evidence for the involvement of a form of cytochrome P-450, *J. Med. Chem.* 29 (1986) 1596-1603.
- [12] P. Ioan, E. Carosati, M. Micucci, G. Cruciani, F. Broccatelli, B.S. Zhorov, A. Chiarini, R. Budriesi, 1,4-Dihydropyridine Scaffold in Medicinal Chemistry, *The Story so Far And Perspectives (Part 1): Action in Ion Channels and GPCRs*, *Current Medicinal Chemistry* 18 (2011)4901-4922.
- [13] Q. Huang, Y. Li, C. Sheng, Y. Dou, M. Zheng, Z. Zhu, J. Wang, Blood pressure lowering efficacy of amlodipine and nifedipine-Gits in

Siham Aggoun, Salah Belaidi, Lazhar Bouchlaleg, Hassan Nour, Oussama Abchir, Samir Chtita, Muneerah Mogren Almogren, Majdi Hochlaf

- ambulatory hypertension, J. Hypertens, 33 (2015) 94.
- [14] M.F.Gordeev, D.V. Patel, E.M. Gordon, Approaches to the combinatorial synthesis of heterocycles: a solid-phase synthesis of 1,4-dihydropyridines, J.Org.Chem. 61(1996) 924-928.
- [15] B. Hemmateenejad, M.A. Safarpour, R. Miri, F. Taghavi, Application of ab initio theory to QSAR study of 1,4-dihydropyridine-based calcium channel blockers using GA-MLR and PC-GA-ANN procedures, J. Comput. Chem 25(2004) 1495–1503.
- [16] R. Mannhold, B. Jablonka, W. Voigdt, K. Schoenafinger, K. Schraven, Calcium- and calmodulin-antagonism of elnadipine derivatives: comparative SAR, Eur. J. Med. Chem. 27(1992) 229-235.
- [17] L. Yet, 1,4-dihydropyridines. In: Privileged Structures in Drug Discovery. Hoboken, NJ, USA: John Wiley & Sons, Inc 5(2018) 9–82.
- [18] M. Rucins, A. Plotniece, E. Bernotiene, W-B. Tsai, A. Sobolev, Recent Approaches to Chiral 1,4-Dihydropyridines and their Fused Analogues, Catalysts 10 (2020) 1019.
- [19] R. Hanachi, A. Ben Said, H. Allal, S. Rahali, M.A.M. Alkhalifah, F. Alresheedi, B. Tangour, M. Hochlaf, Structural, QSAR, machine learning and molecular docking studies of 5-thiophen-2-yl pyrazole derivatives as potent and selective cannabinoid-1 receptor antagonists, New J. Chem. 45 (2021) 17796-17807.
- [20] M.A. Safarpour, B. Hemmateenejad, R. Miri, M. Jamali, Quantum Chemical-QSAR Study of Some Newly Synthesized 1,4-Dihydropyridine Calcium Channel Blockers. QSAR & Combinatorial Science 22 (2003) 997–1005.
- [21] X. Yao, H. Liu, R. Zhang, M. Liu, Z. Hu, A. Panaye, J.P. Doucet, B. Fan, QSAR and classification study of 1,4-dihydropyridine calcium channel antagonists based on least squares support vector machines, Mol. Pharm. 2 (2005) 348-56.
- [22] F. Hadizadeh, S. Vahdani, M. Jafarpour, Quantitative Structure-Activity Relationship Studies of 4-Imidazolyl- 1,4-dihydropyridines as Calcium Channel Blockers, Iran. J. Basic Med. Sci. 16 (2013) 910-916.
- [23] E.G. Da Mota, D.G. Silva, M.C. Guimarães, E.F.F. da Cunha, M.P. Freitas, Computer-assisted design of novel 1,4-dihydropyridine calcium channel blockers, Mol. Simul. 40 (2014) 959-965.
- [24] C. Jardínez, A. Vela, J. Cruz-Borbolla, R.J. Alvarez-Mendez, J. G. Alvarado-Rodríguez, Reduced density gradient as a novel approach for estimating QSAR descriptors, and its application to 1,4-dihydropyridine derivatives with potential antihypertensive effects, J. Mol. Model. 22(2016) 296.
- [25] T.F. El-Moselhy, P.A. Sidhom, E.A. Esmat, N.A. El-Mahdy, Synthesis, Docking Simulation, Biological Evaluations and 3D-QSAR Study of 1,4-Dihydropyridines as Calcium Channel Blockers, Chem. Pharm. Bull. (Tokyo) 65(2017) 893-903.
- [26] L. Navidpour, R. Miri, A. Shafiee, Synthesis and calcium channel antagonist activity of new 1,4-dihydropyridine derivatives containing lipophilic 4-imidazolyl substituents, Arzneim. Forsch. Drug Res. 54 (2004) 499-504.
- [27] HyperChem (Molecular Modeling System) Hypercube (2008) Gainesville FL 32601, USA
- [28] G. Schneider, K.H. Baringhaus, H. Kubinyi, Molecular Design: Concepts and Applications, John Wiley & Sons, 2008.
- [29] C.A. Lipinski, F. Lombardo, B. W. Dominy, P. Feeney, J. Adv. Drug. Deliv. Rev. 23 (1997) 3-25.
- [30] D.F. Veber, S.R. Johnson, H.Y. Cheng, B.R. Smith, K.W. Ward, K.D. Kopple, Molecular Properties That Influence the Oral Bioavailability of Drug Candidates, J. Med. Chem. 45 (2002) 2615-2623.
- [31] A.K. Ghose, V.N. Viswanadhan, J.J. Wendoloski, J. Comb. Chem 1 (1999) 55.
- [32] M. Ouassaf, S. Belaidi, S. Khamouli, H. Belaidi, S. Chtita, Combined 3D-QSAR and molecular docking analysis of thienopyrimidine derivatives as staphylococcus aureus inhibitors, Acta. Chim. Slov. 68 (2021) 289–303.
- [33] M. Ouassaf, S. Belaidi, K. Lotfy, K.I. Daou, H. Belaidi, Molecular docking studies and ADMET properties of new

Siham Aggoun, Salah Belaidi, Lazhar Bouchlaleg, Hassan Nour, Oussama Abchir, Samir Chtita, Muneerah Mogren Almogren, Majdi Hochlaf

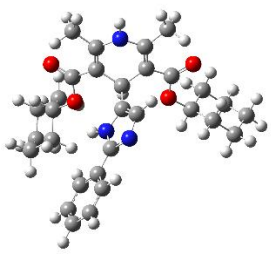
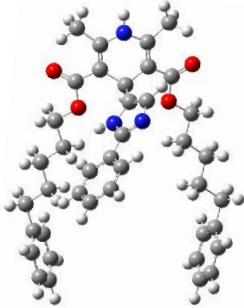
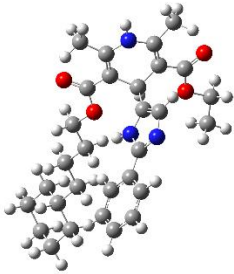
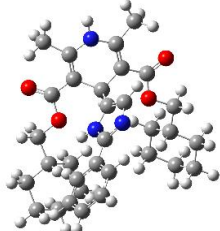
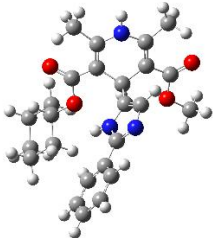
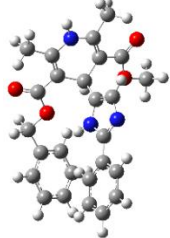
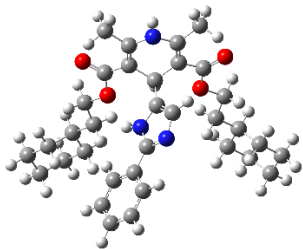
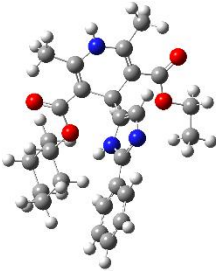
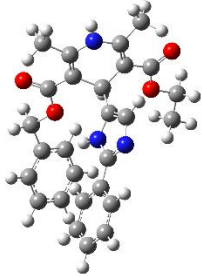
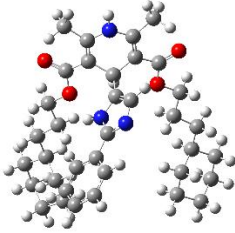
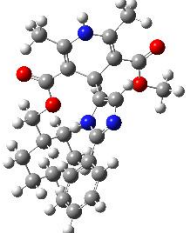
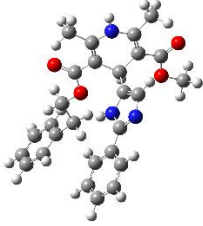
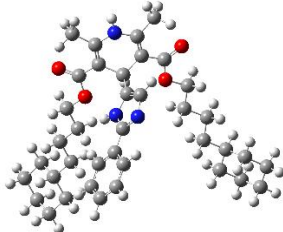
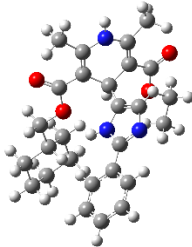
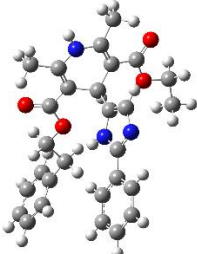
- 1.2. 3 triazole derivatives for anti-breast cancer activity, *J. Bionanosci.* 12 (2018) 1-11.
- [34] ADT / AutoDockTools — AutoDock. <http://autodock.scripps.edu/resources/adt> (Accessed : 28.05. 2022).
- [35] M.D.Hanwell, D.E. Curtis, D.C. Lonie, T. Vandermeersch, E. Zurek, G.R.Hutchison, Avogadro: an advanced semantic chemical editor, visualization, and analysis platform,” *J. Cheminform* 17 (2012) 4.
- [36] BIOVIA Discovery Studio - BIOVIA - Dassault Systèmes®.
- [37] M.J. Frisch, G.W. Trucks, H.B. Schlegel, G.R. Scuseria, M.A. Robb, J.R. Cheeseman, G. Scalmani, V. Barone, B. Mennucci, G.A. Petersson, H. Nakatsuji, M. Caricato, X. Li, H.P. Hratchian, A.F. Izmaylov, J. Bloino, G. Zheng, J.L. Sonnenberg, M. Hada, M. Ehara, K. Toyota, R. Fukuda, J. Hasegawa, M. Ishida, T. Nakajima, Y. Honda, O. Kitao, H. Nakai, T. Vreven, J.A. Montgomery, J.E. Peralta, F. Ogliaro, M. Bearpark, J.J. Heyd, E. Brothers, K.N. Kudin, V.N. Staroverov, R. Kobayashi, J. Normand, K. Raghavachari, A. Rendell, J.C. Burant S.S. Iyengar, J. Tomasi, M. Cossi, N. Rega, J.M. Millam, M. Klene, J.E. Knox, J.B. Cross, V. Bakken, C. Adamo, J. Jaramillo, R. Gomperts, R.E. Stratmann, O. Yazyev, A.J. Austin, R. Cammi, C. Pomelli, J.W. Ochterski, R.L. Martin, K. Morokuma, V.G. Zakrzewski, G.A. Voth, P. Salvador, J.J. Dannenberg, S. Dapprich, A.D. Daniels, O. Farkas, J.B. Foresman, J.V. Ortiz, J. Cioslowski, D.J. Fox, (2009) Gaussian 09, revision D.01. Gaussian Inc, Wallingford
- [38] M.Alloui, S. Belaidi, H. Othmani, N.E. Jaidane, M.Hochlaf, Imidazole derivatives as angiotensin II AT1 receptor blockers : Benchmarks, drug-like calculations and quantitative structure-activity relationships modeling, *Chem. Phys. Lett.* 696 (2018) 70–78.
- [39] S.Boudergua, M. Alloui, S. Belaidi, M. Mogren, U.A Al Mogren, Abd Ellatif Ibrahim, M. Hochlaf, QSAR Modeling and Drug-Likeness Screening for Antioxidant Activity of Benzofuran Derivatives, *J. Mol. Struct.* 1189 (2019) 307-314.
- [40] M. Ghamri, D. Harkati ,S. Belaidi, S. Boudergua, R. Linguerra, G. Chambaud, M. Hochlaf, Carbazole derivatives containing chalcone analogues targeting topoisomerase II inhibition: first principles characterization and QSAR modeling. *Spectrochim. Acta A* 242 (2020) 118724.
- [41] I. Almi, S. Belaidi, A. Zerroug, M. Alloui, R. Ben Said, R. Linguerra, M. Hochlaf, QSAR investigations and structure-based virtual screening on a series of nitrobenzoxadiazole derivatives targeting human glutathione-S-transferases. *J. Mol. Struct.* 1211 (2020) 128015.
- [42] M. Manachou, Z. Gouid, Z. Almi, S. Belaidi, S. Boughdiri, M. Hochlaf, Pyrazolo[1,5- a][1,3,5] triazin-2thioxo-4-ones derivatives as thymidine phosphorylase inhibitors: Structure, drug-like calculations and quantitative structure-activity relationships (QSAR) modeling, *J. Mol. Struct.* 1199 (2020) 127027.
- [43] S.Chtita, M. Ghamali, R. Hmamouchi, B. Elidrissi, B. Bourass, M. Larif, M. Bouachrine, T. Lakhli, Investigation of Antileishmanial Activities of Acridines Derivatives against Promastigotes and Amastigotes Form of Parasites Using Quantitative Structure Activity Relationship Analysis, *Advances in Physical Chemistry* 5137289(2016) 16.
- [44] D. Eros, I. Kövesdi, L.Orfi, K. Takács-Novák, GY. Acsády, Gy. Kéri, Reliability of logP predictions based on calculated molecular descriptors: a critical review, *Curr. Med. Chem.* 9 (2002) 1819-29.
- [45] A. Ambati, C.S. Canakis, J.W. Miller, E.S. Gragoudas, E. Edwards, D.J. Weissgold, I. Kim, F.C. Delori, A.P. Adamis, Diffusion of High Molecular Weight Compounds through Sclera, *Investig. Ophthalmol. Vis. Sci.* 41 (2000) 1181-1185.
- [46] C.A. Lipinski, F. Lombardo, W. Dominy, P. Feeney, Experimental and computational approaches to estimate solubility and permeability in drug discovery and development settings, *J. Adv. Drug Deliv. Rev.* 46 (2001) 3-26.
- [47] A. Zerroug, S. Belaidi, I. BenBrahim, L. Sinha, S. Chtita, Virtual screening in drug-likeness and structure/activity relationship of pyridazine derivatives as Anti-Alzheimer drugs, *J. King Saud Univ. Sci.* 31 (2019) 595-601.
- [48] G. Schaftenaar, J. deVlieg, *J. Comput. Aided Mol.Des* 26 (2012) 311–318.

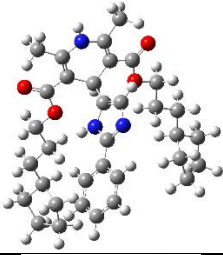
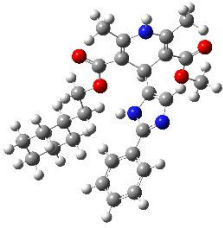
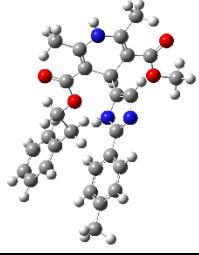
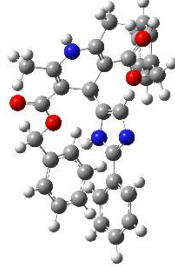
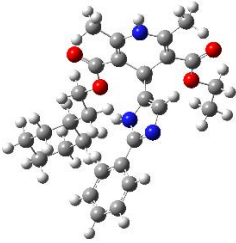
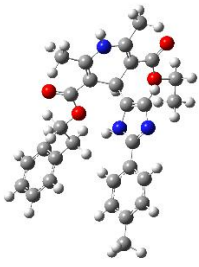
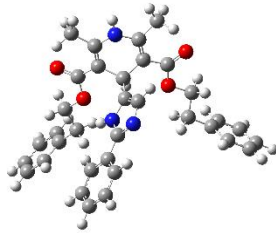
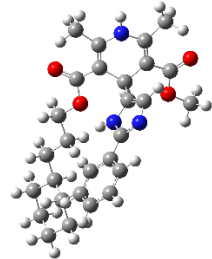
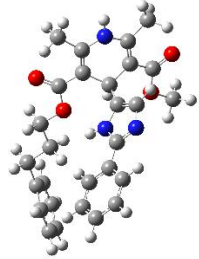
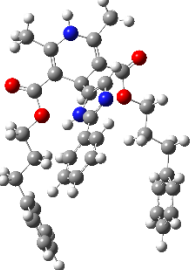
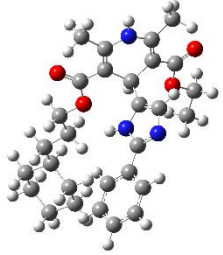
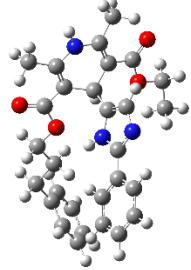
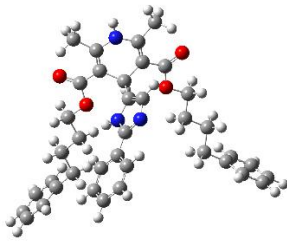
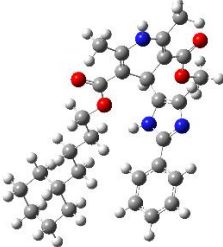
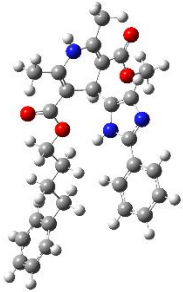
Siham Aggoun, Salah Belaidi, Lazhar Bouchlaleg, Hassan Nour, Oussama Abchir, Samir Chtita, Muneerah Mogren Almogren, Majdi Hochlaf

- [49] K. Dermeche, N. Tchouar, S. Belaidi, T. Salah, Qualitative Structure-Activity Relationships and 2D-QSAR Modeling of TNF- α Inhibition by Thalidomide Derivatives, *J. Bionanosci.* 9 (2015) 395-400.
- [50] A. Kerassa, S. Belaidi, D. Harkati, T. Lanez, O. Prasad, L. Sinha, Investigations on Molecular Structure, Electronic Properties, NLO Properties and Comparison of Drug-Likeness of Triazolothiadiazole Derivatives by Quantum Methods and QSAR Analysis, *Rev. Theor. Sci.* 4 (2016) 85-96.
- [51] A. Mauri, V. Consonni, R. Todeschini, Handbook of Computational Chemistry, Springer, Cham, (2017) 2065-2093.
- [52] XLSTAT software, XLSTAT Company. <https://www.xlstat.com>.
- [53] MATLAB 7.9.0 (R2009b) and Statistics Toolbox Release, the Math Works, Inc., Natick, Massachusetts, United States, 2011.
- [54] S. Chtita, M. Ghamali, R. Hmamouchi, M. Larif, M. Bouachrine, T. Lakhlifi, Quantitative structure-activity relationship studies of anticancer activity for Isatin (1H-indole-2,3-dione) derivatives based on density functional, *IJQSPR* 2(2017) 90-115.
- [55] L. Eriksson, J. Jaworska, A.P. Worth, M.T. Cronin, R.M. McDowell, P. Gramatica, Methods for reliability and uncertainty assessment and for applicability evaluations of classification-and regression-based QSARs, *Environ. Health Perspect.* 111 (2003) 1361-1375.
- [56] T.I. Netzeva, A.P. Worth, T. Aldenberg, R. Benigni, M.T. Cronin, P. Gramatica, J.S. Jaworska, S. Kahn, G. Klopman, C.A. Marchant, Current status of methods for defining the applicability domain of quantitative structure-activity relationships. The report and recommendations of ECVAM Workshop 52. *Altern. Lab. Anim.* 33 (2005) 155-173.
- [57] J. Jaworska, N. Nikolova-Jeliazkova, T. Aldenberg, QSAR applicability domain estimation by projection of the training set in descriptor space, *Altern. Lab. Anim.* 33(2005) 445-459.
- [58] E. Zerroug, S. Belaidi, S. Chtita, Artificial neural network-based quantitative structure-activity relationships model and molecular docking for virtual screening of novel potent acetylcholinesterase inhibitors, *J. Chin. Chem. Soc.* 68 (2021) 1379-1399.
- [59] J. Luo, J. Hu, L. Fu, C. Liu, X. Jin, Use of Artificial Neural Network for a QSAR Study on Neurotrophic Activities of N-p-Tolyl/phenylsulfonyl L-Amino Acid Thiiolester Derivatives, *Procedia Eng.* 15(2011) 5158-5163.
- [60] L. Terfloth, J. Gasteiger, Neural networks and genetic algorithms in drug design, *DDT* 6(2001) 102-108.
- [61] F. Cheng, V. Sutariya, Applications of Artificial Neural Network Modeling in Drug Discovery, *Clin. Exp. Pharmacol.* 2(2012) 113.
- [62] B.D. Ripley, Pattern Recognition and Neural Networks, Cambridge University Press, NY United States, USA, 1996.

SUPPLEMENTAL INFORMATION

Table S1. 3D Chemical structures of 1, 4-dihydropyridines derivatives under study (Table 1).

NO	Compound structure	NO	Compound structure	NO	Compound structure
1		11		21	
2		12		22	
3		13		23	
4		14		24	
5		15		25	

6		16		26	
7		17		27	
8		18		28	
9		19		29	
10		20		30	
	31	